Extreme high rotational excitation of ClO

Robert Aures,[a] Karl-Heinz Gericke,*[a] Masahiro Kawasaki,[b] Christof Maul,[a] Yukio Nakano,[b] Gundula Trott-Kriegeskorte[a] and Zhenya Wang[c]

[a] Institut für Physikalische und Theoretische Chemie, Technische Universität Braunschweig, Hans-Sommer-Straße 10, D-38106 Braunschweig, Germany. E-mail: k.gericke@tu-bs.de; Fax: 49 531 391 5396; Tel: 49 531 391 5326
[b] Department of Molecular Engineering, Kyoto University, Kyoto 606-8501, Japan
[c] Laboratory of Laser Spectroscopy, Academia Sinica, 230031 Hefei, People's Republic of China

We observed the population of extremely high non-thermal rotational states of ClO ($J_{max} = 130.5$) upon photodissociation of Cl_2O. State-resolved and isotope-specific detection of nascent ClO is performed by observing single colour $(2 + 1)$ resonance enhanced multiphoton ionisation (REMPI) spectra following excitation in the wavelength range from 336 to 344 nm. The REMPI spectrum is assigned to the $ClO(C^2\Sigma^-, v' = 0 \leftarrow X^2\Pi_\Omega, v = 0)$ transition. The non-thermal population of rotational states is highly inverted, peaking at $J = 107.5$. The photodissociation of Cl_2O is a classical example for the pure impulsive model, as a consequence of the Cl_2O mass distribution and a weak dependence of the upper potential energy surface on the bond angle. Cl_2O can thus be used as clean source for laboratory generation of highly excited ClO molecules with a defined non-thermal rotational population. In kinetic studies using ClO from Cl_2O as precursor the high rotational excitation needs to be considered carefully.

Introduction

Highly rotationally excited states of small (diatomic) molecules reflecting Boltzmann (thermal) or non-thermal state populations have been observed in the cosmos and high altitudes of our atmosphere,[1] though few accounts for laboratory generated highly rotationally excited molecules can be found in the literature. Iodine is thermally populated up to $J = 200$, yet the ensemble of molecules with $J > 100$ makes up only 16%. Cossart-Magos and Cossart observed non-thermal distributed CO excited up to $J = 120$ in a cooled electric discharge.[2] The maximum of the rotational distribution of N_2 from the photodissociation of N_2O can be found at $J = 74$.[3–5] Hanisco and Kummel reported for the photodissociation of N_2O around 202 nm an average rotational energy of N_2 of 1.4 eV, i.e. 57% of the available energy.[3] Tanaka et al. have observed high rotational excitation upon photodissociation of Cl_2O at 235 nm.[6] For laboratory production of highly rotationally excited species via photodissociation a bent molecule of type A–B–A is favoured, with $m_A \gg m_B$. Such an intramolecular mass distribution will induce high rotation in the molecule AB upon fragmentation. Therefore, Cl_2O is an ideal candidate for the laboratory generation and observation of high rotational states of ClO. Using the resonance enhanced multiphoton ionisation (REMPI) method to study the photofragmentation of Cl_2O one is able to distinguish between signals from the two prominent ClO isotopes (^{35}ClO and ^{37}ClO).[7] Thus, isotopically pure spectra can be observed, greatly simplifying the complex ClO spectra and facilitating their interpretation.

The present paper describes the generation of extremely rotationally excited ClO from the photodissociation of Cl_2O in the wavelength range from 336 to 344 nm. For the first time, for the photodissociation of Cl_2O, isotope selective spectra for ^{35}ClO and ^{37}ClO are measured. The ClO fragment is completely characterised by its rotational and spin–orbit states using $(2 + 1)$ REMPI. Using computer simulation the highly inverted non-thermal rotational state population of ClO is determined.

Experimental

ClO is studied in a one-colour experiment consisting of two elementary steps. First, Cl_2O is dissociated by absorbing one UV photon (between 336 nm and 344 nm). The resulting ClO fragment is then detected via a $(2 + 1)$ REMPI process.[8,9] Ground state ClO $(X^2\Pi_\Omega, \Omega = {}^1/_2, {}^3/_2, v = 0, J)$ is excited to the upper electronic C state $(C^2\Sigma^- v' = 0, J' \leftarrow X^2\Pi_\Omega, v = 0, J)$ by absorption of two UV photons and subsequently ionised by one photon. Both the Cl_2O photolysis wavelength and the ClO detection wavelength were delivered by the same tuneable dye laser (FL 3002, Lambda Physik) pumped by a XeCl excimer laser (Radiant Dyes RD-EXC-200). The experimental set-up, including the linear time-of-flight (TOF) spectrometer, is described in detail elsewhere.[10] Briefly, it consists of a vacuum chamber evacuated to a base pressure of 10^{-6} mbar where a pulsed supersonic gas jet is crossed by the laser beam. Ionised fragments are accelerated towards a double-stage multichannel plate assembly where the signal is read out to a digital oscilloscope and integrated by a boxcar averager. Isotope-specific spectra were observed simultaneously by adjusting two boxcar gates at the respective arrival times of ^{35}ClO and ^{37}ClO while scanning the dye laser. For the preparation of gaseous dichlorine monoxide (Cl_2O) the method of Cady[11] was used.

Results and discussion

An overview over the observed ^{35}ClO REMPI spectra resulting from the one-colour experiment in the dissociation of Cl_2O is represented in Fig. 1. The upper part (a) of the figure shows a spectrum for both spin–orbit manifolds of the ^{35}ClO isotope, the lower part (b) shows a simulated spectrum for the
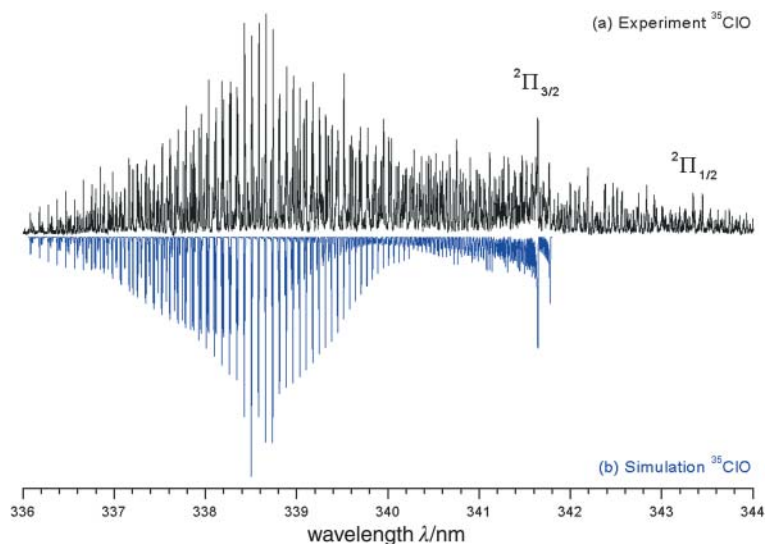
Fig. 1 Experimental (a) and simulated (b) excitation spectra of ^{35}ClO in the one-colour photodissociation study of Cl_2O between 336 and 344 nm: $ClO(X^2\Pi_{1/2,3/2}, v = 0) + 2\,h\nu \rightarrow ClO(C^2\Sigma^-, v' = 0)$. For the simulated spectra (b) only the rotational branches of the $^2\Pi_{3/2}$ spin-manifold are given. Molecular constants for the simulation were taken from ref. 12, 15, 16.

$^2\Pi_{3/2}$ spin–orbit system of the ^{35}ClO isotope for reference. The scan range from 336 nm to 344 nm covers the rotational branches of $ClO(C^2\Sigma^-, v' = 0 \leftarrow X^2\Pi_{3/2}, v = 0)$ and $ClO(C^2\Sigma^-, v' = 0 \leftarrow X^2\Pi_{1/2}, v = 0)$. The onset of the $^2\Pi_{3/2}$ system at 341.6 nm in the figure is indicated by the band heads of the P and O branches. The other spin–orbit system, $^2\Pi_{1/2}$, starts at about 343.6 nm. At room temperature both electronic systems are well separated (spin–orbit coupling constant $A_O = -321.79$ cm^{-1}).[12] In the Cl_2O dissociation, due to the high rotational excitation, transitions from high rotational states of the $^2\Pi_{1/2}$ system overlap with transitions from the $^2\Pi_{3/2}$ system. High rotational excitation is also present in excited vibrational states of ClO obscuring the bandheads of the $^2\Pi_{1/2}$ system at 343.6 nm in the overview of Fig. 1. The complex spectrum of the two-photon (0–0) transition in Fig. 1 consists of 20 main and satellite branches. Regarding the smallness of the spin-splitting constant $\gamma = -0.0129$ cm^{-1} of the upper $C^2\Sigma^-$ state, the one-photon laser linewidth of 0.2 cm^{-1} and the intensity ratios for main and satellite lines it is expected that the satellite lines are only resolvable for high J quanta ($J > 30$). Neglecting the overlap of the $^2\Pi_\Omega$ spin manifolds, the spectrum below 341.6 nm ($^2\Pi_{3/2}$ bandhead) is contributed to by ten resolvable branches, namely the $^OO_{11}$, $^PP_{11}(^PO_{21})$, $^qQ_{11}(^qP_{21})$, $^rR_{11}(^rQ_{21})$, $^sS_{11}(^sR_{21})$ and $^tS_{21}$ branches. The satellite branches overlapping with the respective main branches (for $J < 30$) are given in parentheses (notation $^{\Delta N}\Delta J_{F'F''}$). The Q branch intensities for two-photon $^2\Sigma \leftarrow ^2\Pi$ transitions are negligibly small.[13,14] The simulation used was generated using the molecular constants given in Table 1[15,16] and calculated Hönl–London factors.[13,14] The agreement between the simulation and the experiment is excellent. Note the contribution of the high J transitions of the overlapping $^2\Pi_{1/2}$ spin system.

The simulated ^{35}ClO spectrum was obtained by fitting the centrifugal constant D and the sextic centrifugal constant H of the upper state $^2\Sigma^-$, assuming that the constants for the ground state $^2\Pi_{3/2}$ and the rotational constant B of the upper state are well known.[12,15,16] For the calculation of the energy levels of the $^2\Pi$ state the formula from Sheasley and Matthews was used.[17] A least squares fit of the simulation to the experimental spectrum yielded for the C state the values 1.12933×10^{-6} cm^{-1} for D_0 and -2.56×10^{-13}cm^{-1} for H_0. The population of the rotational states (*cf.* Fig. 2) was extracted from the simulated spectra.

It shows a Gaussian distribution peaking at $J = 107.5$, with a full width at half maximum (FWHM) of $\Delta J = 26.6$. The

distribution $P(J)$ is strongly inverted and ClO is essentially formed in rotational states above $J = 90$. The graph clearly depicts that about 71% of the total rotational population of ClO is situated in between the FWHM limits of the distribution [$94.5 < J < 120.5$]. Such extremely high rotational states (up to $J = 130$) in a diatomic have never been observed in the laboratory before. The low J population ($J < 30$) is due to ClO

Table 1 Molecular constants for $^{35}Cl^{16}O^a$

$^{35}Cl^{16}O$	$^2\Pi_{3/2}$	$^2\Sigma^-$
B_0/cm^{-1}	0.620505704^b	0.6952^c
D_0/10^6 cm^{-1}	1.328^b	1.71^c
H_0/10^{13} cm^{-1}	-5.00^b	—
A/cm^{-1}	-320.31494^b	—
A_D/cm^{-1}	9.7216455^b	—
γ/10^2 cm^{-1}	—	-1.29^c
p_0/10^2 cm^{-1}	-2.2552569^b	—
q_0/10^5 cm^{-1}	3.34898^b	—
ω_e/cm^{-1}	853.72446^b	1077.74^d
$\omega_e x_e$/cm^{-1}	5.579573^b	6.365^d

^{a}B: rotational constant, D: centrifugal distortion, H: sextic centrifugal distortion, A: spin–orbit coupling constant, A_D: centrifugal distortion of A, γ: spin rotation coupling constant, p_o: lambda doubling constant, q_o: lambda doubling constant, ω_e: vibrational constant, x_e: anharmonic constant. ^{b}Ref. 15, 16. ^{c}Ref. 12. ^{d}Ref. 16.
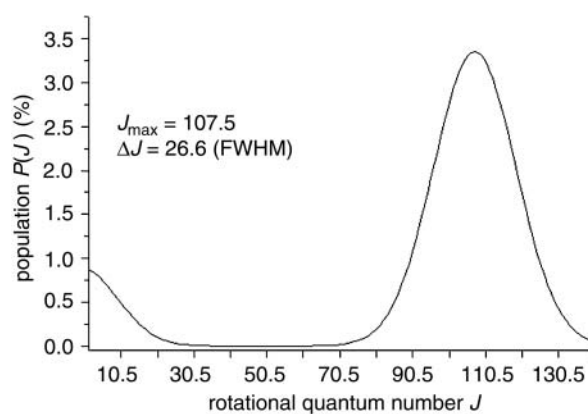

Fig. 2 Strongly inverted rotational state distribution of ^{35}ClO($v = 0$) generated in the photodissociation of ClOCl around 340 nm. The data were extracted from a fit to the experimental spectrum (*cf.* Fig. 1).

originating from the photodissociation of ClO_2 which is always present as a small impurity (1%) in Cl_2O samples[18] and is characterised by a Boltzmann distribution with a temperature parameter of 650 K.[19] For the fit it was assumed that the signal intensity depends on the third power of the laser intensity, since the transitions using two photons in the REMPI scheme and the fragmentation were not saturated, whereas the final ionisation was. In principle, there are three possible sources for the observed high rotational excitation: Overall rotation of the parent molecule in the electronic ground state, bending vibration within the parent molecule, and finally, the torque generated by the anisotropy of the upper potential energy surface (PES), *i.e.* exit channel dynamics. The influence of the first effect can be excluded, since our experiments were measured under molecular beam conditions ($T_{rot} < 10$ K). The effect of zero-point vibration of the bending mode of Cl_2O on the rotational distribution of ClO has been calculated to be smaller than ten rotational quanta around the maximum of $J = 107.5$. Dynamic induction of rotational energy onto the diatomic fragment generated from the photodissociation of a triatomic parent molecule must be viewed in Jacobi coordinates r, R, and γ. Here, r is the internuclear distance in the diatomic, characterising vibrational excitation, R is the distance between the atomic fragment and the centre of mass of the diatomic characterising the separation dynamics, hence the translational energy of the system, and γ denotes the angle of r with R, thus characterising the rotation of the diatomic. For ClO the Jacobi coordinates r, R and γ are related to the natural coordinates (r_{ClO}, $r_{Cl'O}$) and α:

$$r = r_{ClO} \tag{1}$$

$$R = (r_s^2 + r_{Cl'O}^2 - 2 r_s r_{Cl'O} \cos\alpha)^{0.5} \tag{2}$$

$$\gamma = \arcsin(r_{Cl'O} R^{-1} \sin\alpha) \tag{3}$$

where r_{ClO} and $r_{Cl'O}$ are the distances between the central O atom and the terminating Cl atoms, r_s is the distance between the central O atom and the centre of mass of the ClO diatom and α is the bond angle. Cl′ denotes the departing atom whereas Cl remains bound to O in the ClO fragment. The amount of rotational excitation can be evaluated by integrating the gradient $F_\gamma = -(\partial V/\partial\gamma)$ of the upper PES along the dissociation coordinates in natural coordinates. Then F_γ can be separated into two parts:[20]

$$F_\gamma = -\left(\frac{\partial V}{\partial r_{Cl'O}}\right)\left(\frac{\partial r_{Cl'O}}{\partial\gamma}\right) - \left(\frac{\partial V}{\partial\alpha}\right)\left(\frac{\partial\alpha}{\partial V}\right) = F_\gamma^{(1)} + F_\gamma^{(2)} \tag{4}$$

where the first part $F_\gamma^{(1)}$ describes the rotational excitation induced by the impulsive model[21] where any PES dependence on bond angle α is neglected. Often the dynamic part $F_\gamma^{(2)}$, *i.e.* the bond angle dependence of the upper PES, dominates the rotational angular momentum transfer onto the diatomic products. However, especially for a triatomic parent molecule with a light central and two heavy terminating atoms like Cl_2O the impulsive part $F_\gamma^{(1)}$ becomes more important due to a large value of $(\partial r_{Cl'O}/\partial\gamma)$. If no data are known for the upper PES the so-called pure impulsive model can be used to describe the amount of rotational excitation of the fragment.[20] In the case of the ClOCl molecule this model assumes that the O–Cl bond breaks instantaneously with Cl merely playing the role of a spectator. The sudden repulsion between Cl and O–Cl generates a torque which induces rotation of O–Cl about its centre of mass. The rotational energy of the fragment E_{rot} is related to the excess energy E_{exc} by

$$E_{rot} = E_{exc} \frac{m_{Cl}^2 \sin^2\alpha_0}{m_{ClO}^2 - m_{Cl}^2 \cos^2\alpha_0} \tag{5}$$

where $E_{exc} = h\nu - D_0$ is given by the difference of the photon energy of the dissociating laser and the dissociation energy D_0, m_{Cl} and m_{ClO} are the atomic masses of the fragments and α_0 is the initial Cl–O–Cl bond angle at the time when the O–Cl bond breaks. If α_0 is chosen to be the equilibrium angle in the electronic ground state, eqn. (5) defines the most probable final angular momentum state of the fragment, using the simple relation $E_{rot} = B_{rot} J(J + 1) - D_{rot}(J(J + 1))^2$. In our case ($\alpha_0 = 110.886°$) the pure impulsive model yields for the excess energy of 2.2 eV a value of 0.96 eV for E_{rot}, respectively $J = 112.5$, *i.e.* the rotational energy is about 44% of E_{exc}. With respect to the rotational population derived from the experiments, peaking at $J = 107.5$, Cl_2O can therefore be seen as a classical example of a molecule showing high non-thermal rotational excitation upon photodissociation. The observed width of the rotational distribution $\Delta J = 26.6$ (FWHM) is likely due to dynamical effects on the PES other than discussed above.

Conclusion

For the first time isotope- and state-specific spectra of ClO generated in the near UV photodissociation of Cl_2O have been measured by one-colour (2 + 1) REMPI under background-free conditions. A narrow non-thermal population of extremely high rotational states of the diatomic ClO has been observed opening up the possibility to use the Cl_2O photodissociation as a clean source for high angular momentum diatomics. The high rotational excitation induced in the Cl_2O photodissociation is a typical case for a pure impulsive fragmentation model. The high rotational excitation of ClO obtained from Cl_2O as precursor needs carefully to be considered in kinetics studies involving the ClO radical.

Acknowledgements

References

1 B. Hubert, J.-C. Gérad, V. I. Shematovich and D. V. Bisalko, *Geophys. Res. Lett.*, 1996, **23**(17), 2215.
2 C. Cossart-Magos and D. Cossart, *J. Chem. Phys.*, 2000, **112**, 2148.
3 T. F. Hanisco and A. C. Kummel, *J. Phys. Chem.*, 1993, **97**, 7242.
4 D. W. Neyer, A. J. R. Heck, D. W. Chandler, J. M. Teule and M. H. M. Janssen, *J. Phys. Chem.*, 1999, **103**, 10388.
5 J. M. Teule, G. C. Groenenboom, D. W. Neyer, D. W. Chandler and M. H. M. Janssen, *Chem. Phys. Lett.*, 2000, **320**, 177.
6 Y. Tanaka, M. Kawasaki, Y. Matsumi, H. Fujiwara, T. Ishiwata, L. R. Rogers, R. N. Dixon and M. N. R. Ashfold, *J. Chem. Phys.*, 1998, **109**, 1315.
7 M. J. Cooper, T. Diez-Rojo, L. J. Rogers, C. M. Western, M. N. R. Ashfold and J. W. Hudgens, *Chem. Phys. Lett.*, 1997, **272**, 232.
8 E. Rühl, A. Jefferson and V. Vaida, *J. Phys. Chem.*, 1990, **94**(7), 2990.
9 M. Roth, C. Maul and K.-H. Gericke, *J. Chem. Phys.*, 1997, **107**(24), 10582.
10 T. Haas, K.-H. Gericke, C. Maul and F. J. Comes, *Chem. Phys. Lett.*, 1993, **108**, 202.
11 G. H. Cady, *Inorg. Synth.*, 1957, **5**, 156.
12 J. A. Coxon, *Can. J. Phys.*, 1979, **57**, 1538.
13 J. B. Halpern, H. Zacharias and R. Wallenstein, *J. Mol. Spectrosc.*, 1980, **79**, 1.
14 J. O. Hornkohl and W. M. Ruyten, *J. Mol. Spectrosc.*, 1987, **123**, 499.
15 J. B. Burkholder, P. D. Hammer, C. J. Howard, A. G. Maki, G. Thompson and C. Chackerian, *J. Mol. Spectrosc.*, 1987, **124**, 139.

16 A. G. Maki, F. J. Lovas and W. B. Olson, *J. Mol. Spectrosc.*, 1982, **92**, 410.

17 W. D. Sheasley and C. W. Matthews, *J. Mol. Spectrosc.*, 1973, **72**, 420.

18 M. Roth, Thesis, *Untersuchung photoinduzierter Dreikörperzerfälle am Beispiel von Cl₂O und SOCl₂*, dissertation.de, Berlin, 2001.

19 S. Baumgärtel and K.-H. Gericke, *Chem. Phys. Lett.*, 1994, **227**, 461.

20 R. Schinke, *Photodissociation Dynamics*, Cambridge University Press, Cambridge, 1993.

21 G. E. Busch and K. R. Wilson, *J. Chem. Phys.*, 1972, **56**, 3626.